

SYNTHESIS AND PROPERTIES OF INORGANIC COMPOUNDS

Synthesis and Properties of LiNiO_2 Close to Stoichiometric Composition

Obtained by Combined Synthesis Method

R. I. Korneykov^{a, b}, V. V. Efremov^{a, c, *}, S. V. Aksanova^b, K. A. Kesarev^b, O. I.

Akhmetov^a, O. B. Shcherbina^b, I. R. Elyzарova^c, I. G. Tananaev^b, O. O.

Shichalin^a

^a*Sakhalin State University, Yuzhno-Sakhalinsk, 693000 Russia*

^b*Institute of Chemistry and Technology of Rare Elements and Mineral Raw Materials, Apatity, 184209 Russia*

^c*Institute of Industrial Problems of the North Ecology, Apatity, 184209 Russia*

*e-mail: v.efremov@ksc.ru

Received October 29, 2024

Revised November 16, 2024

Accepted November 19, 2024

This study presents the synthesis and characterisation of lithium nickelate LiNiO_2 with near-stoichiometric composition prepared by a combined method. LiNiO_2 exhibits high electrochemical properties including a theoretical capacity of 250-270 mA/g, making it a promising cathode material for lithium-ion batteries as an alternative to LiCoO_2 . However, the commercial use of LiNiO_2 is limited by the difficulty in achieving stoichiometric composition and the high cost of conventional synthesis methods. Using X-ray phase analysis and spectrometry, we identified the phases formed and determined their chemical composition. Electron microscopy and Brunauer-Emmett-Teller (BET) techniques were used to investigate the structure and morphology. The developed process scheme led to the preparation of lithium nickelate with the composition $\text{Li}_{(0.98)}\text{Ni}_{(1.02)}\text{O}_2$, providing the formation of nanoscale samples with high specific surface area and improved electrochemical performance. These results emphasise the potential of LiNiO_2 as a competitive cathode material for lithium-ion batteries.

Keywords: lithium-ion batteries, cathode, lithium nickelate, sol-gel, solid-phase synthesis

DOI: 10.31857/S0044457X250105e3

INTRODUCTION

Nickel compounds are used as electrode materials in batteries, for example in the form of $\text{NiO}(\text{OH})$ in Ni-Cd и Ni-MH. Despite the fact that about LiNiO_2 has been

known since the early 1950s [1], and it has only recently come to be considered as a promising cathode material for lithium-ion batteries [2].

It is widely known that the electrochemical characteristics of any battery depend on the characteristics of the cathode material used [3]. Thus, materials based on phosphates and oxides are used in battery systems [4, 5]. However, the use of oxides as cathode materials is considered more preferable [6–8]. Transition metal oxides with a spinel structure similar to the LiMn structure are widely used in commercial lithium batteries, LiMn_2O_4 , and a layered structure with the general formula LiMO_2 (M = Co and Ni) [4, 9, 10]. Given that LiCoO_2 and LiMn_2O_4 have similar electrochemical properties, only LiCoO_2 has found wide application, despite its high cost and toxicity to both humans and the environment [11]. In addition, LiCoO_2 cathodes are thermally unstable and explosive in batteries, especially in large power sources such as electric vehicles [7, 12]. The main reason why LiMn_2O_4 has not found wide application in commercial lithium batteries as a cathode material, this is the Yang effect–Teller (significant decrease in cell capacity during the charge-discharge process) [13–15].

High thermal stability, the number of charge-discharge cycles, and safety make LiFePO_4 a suitable cathode and a good replacement for traditional LiCoO_2 . However, it has the problem of poor ionic and electron conductivity. Which was eliminated by alloying with Fe metal, carbon coating and mixing LiFePO_4 with conductive materials to improve conductivity [16]. Despite this, the LiFePO_4 battery has a limited capacity of 170 mA/g, which is much lower than the capacity of lithium-ion batteries using transition metal oxides as cathode materials. In addition, the disadvantages of this type of battery include: low operating voltage of 3.2 V and minimum operating voltage (discharge) of 2.5 V [17].

Thus, the existing disadvantages of commercial lithium-ion batteries using LiCoO_2 , LiMn_2O_4 , LiFePO_4 as cathodes make the study of LiNiO_2 as a cathode relevant. Electrochemical studies have demonstrated that it has advantages over other

cathode materials: high theoretical capacity of 250-270 mA/g [18], long service life with insignificant capacity decrease, deep discharge below 2 V [19]. At elevated temperatures, LiNiO_2 and LiCoO_2 undergo a phase transition from hexagonal to cubic phase, with the hexagonal phase being electrochemically active and the cubic phase being inactive. For LiCoO_2 , the phase transition is reversible, while for LiNiO_2 , it is only partially reversible. This means that the only disadvantage of LiNiO_2 is that the synthesis process is complex and requires extreme caution. As a result, two problems may arise: cation mixing and stoichiometry violation. Additionally, the electrochemical properties of the LiNiO_2 cathode strongly depend on the synthesis conditions, therefore optimization of the conditions for obtaining LiNiO_2 is necessary to minimize negative factors [20]. Obviously, research on finding new synthesis methods and optimizing synthesis conditions for LiNiO_2 , crystal chemistry, and electrochemical properties of LiNiO_2 is relevant and of significant interest, as it will allow obtaining another lithium-ion battery of a different class with a high operating voltage of 4 V. Such studies are conducted to understand the correlation between the physical and electrochemical properties of LiNiO_2 and to obtain nickel-based cathode systems with superior characteristics for lithium and lithium-ion cells.

Usually, to obtain LiNiO_2 close to stoichiometric composition, multi-operational approaches are used, which involve long-term thermal treatment (5-25 hours), expensive oxidants, particularly pure oxygen, and pressure different from atmospheric, which is complex in hardware implementation and energy-intensive [21-23].

The aim of the work is to find an alternative synthesis method and determine the optimal conditions for synthesizing cathode materials based on lithium nickelate close to stoichiometric composition, as well as to study the electrochemical properties and physical parameters of the obtained compounds.

EXPERIMENTAL PART

The synthesis of the cathode material LiNiO_2 was carried out by combining the sol-gel method and solid-phase approach. Lithium hydroxide monohydrate (purity 99.00%, Nevareaktiv, Russia) and nickel chloride hexahydrate (purity 97%, Nevareaktiv, Russia) were used. The compounds were dissolved in deionized water to the required concentration. Sodium hypochlorite (purity 99%, Nevareaktiv, Russia) was also used as a ready-made solution.

X-ray phase analysis of the washed synthesized compounds was performed on a Rigaku MiniFlex 600 multifunctional X-ray diffractometer ($\text{Cu } K\alpha$ -radiation) with SmartLab Studio II software (Rigaku Japan), which is a multipurpose device designed for qualitative and quantitative phase analysis of polycrystalline materials. The instrument software allows determining the crystallite size and level of crystal lattice distortions, refining lattice parameters, and conducting material structure refinement using the Rietveld method. ICDD, PDF-4+ 2021 databases were used for phase identification.

To determine the elementary chemical composition, measurements were performed on an ELAN 9000 DRC-e mass spectrometer (Perkin Elmer, USA) with inductively coupled argon plasma with a closed cooling system, with sample introduction using a peristaltic pump and an AS-93+ autosampler.

Identification of the obtained lithium nickelate samples was carried out by IR spectroscopy. IR absorption spectra of lithium nickelate samples in KBr tablets (manufactured by Specac, medium for IR spectroscopy, UK) were recorded on a single-beam IR spectrophotometer with Fourier transform IRTtracer-100 (Shimadzu Corporation, Japan) in the wavenumber range of 4000-400 cm^{-1} .

The specific surface area of the synthesized calcined washed materials (S_{sp}) was determined by the Brunauer-Emmett-Teller (BET) method using nitrogen

sorption/desorption isotherms on a TriStar II 3020 electronic specific surface area analyzer (Micrometrics, USA).

To study the microstructure of the synthesized lithium nickelate powder particles, a scanning electron microscope SEM LEO-420 (Carl Zeiss, Germany) and the ScanMaster software were used for mathematical processing of the obtained images and making measurements. The program allows selecting individual objects in the image, determining their characteristics, and performing statistical processing of the selected objects according to chosen criteria. The object length was chosen as a criterion – the maximum of the lengths of 18 projections onto the orientation line of the object.

Before studying the electrochemical properties, tablets were formed from the samples in a mold on a hydraulic press 7.11 (Sorokin, Russia) with a force of 1 t/cm². Then the tablets were subjected to heat treatment in a laboratory muffle furnace MIMP-25P. After that, electrodes were applied to the surface of the samples by magnetron sputtering of a thin layer of platinum. The sample with applied electrodes can be considered as a flat capacitor. The measuring cell with the sample was connected to a Solartron-1260 impedance analyzer (AMETEK, Inc. (NYSE:AME), Solartron analytical, USA/UK), and measurements were carried out in the frequency range of 0.1-10⁷ Hz. Analysis of the obtained data was performed using the EIS Spectrum Analyser software (Physico-Chemical Research Institute Belarusian State University).

RESULTS AND DISCUSSION

The synthesis of cathode compounds based on lithium nickelates was carried out in stages using a combination of sol-gel and solid-phase methods. In the first stage, preliminary precipitation of nickel hydroxide Ni(OH)₂ from a chloride solution

was carried out. The process was performed in an excess of lithium hydroxide medium. The ratio of lithium to nickel cations varied. After that, nickel was converted from Ni^{2+} to Ni^{3+} by oxidation with sodium hypochlorite. Sodium hypochlorite was chosen as the oxidizing agent due to its relatively low cost. The process was conducted at room temperature, as sodium hypochlorite undergoes thermal destruction starting from 40°C [24]. After this, hydrodynamic processing was performed at a temperature of 90°C. As a result of this heat treatment, partial water loss occurred. This facilitated the formation of nickel oxyhydroxide (NiOOH) precursor molecules [25].

In the second stage, the resulting suspension was evaporated to a dry residue. The composition of the collective precipitate included: nickel oxyhydroxide, sodium chloride formed as a result of redox reactions. During evaporation, the collective precipitate contained partially carbonized lithium hydroxide formed as a result of the interaction of lithium hydroxide with carbon dioxide from the air. The collective precipitate was calcined at different temperatures to form lithium nickelates of various compositions.

After heat treatment, lithium hydroxide underwent complete carbonization. The calcined precipitate was washed from NaCl and Li_2CO_3 in deionized water with a liquid to solid ratio equal to 100. At this ratio, no hydrolytic destruction of the synthesized compounds occurs. Then the washed material was dried at room temperature. After that, the influence of various factors during synthesis on the final composition of the target products was studied. Specifically, the dependences of the chemical composition and physical parameters of the synthesized compounds on the ratio of metal cations ($\text{Li} : \text{Ni}$), time and temperature factors were investigated. When studying the influence of synthesis parameters for the reliability and reproducibility of results, at least three parallel experiments were conducted to obtain samples at each stage of the research. In each specific case, the results were identical.

Since the obtained compounds are isostructural, the composition of materials, in addition to X-ray phase analysis, was additionally identified by chemical methods.

The influence of the ratio of lithium and nickel cations on the composition of the final product was studied. Lithium nickelates were synthesized with a ratio of Li^+ to Ni^{2+} ranging from $1.5 : 1$ to $10 : 1$ at a synthesis temperature of 700°C for 60 minutes. The choice of synthesis temperature was based on the analysis of literature data, while the choice of time was the starting point in studies on optimizing the conditions for obtaining compounds based on lithium nickelates.

It was shown that with an excess of lithium cations relative to nickel cations equal to 1.5, a lithium-depleted phase of composition $\text{Li}_{0.25}\text{Ni}_{1.75}\text{O}_2$ is formed (Fig. 1a, Table 1). Apparently, such an excess of alkali metal cations during synthesis is insufficient to obtain a sample with a higher content of Li^+ cations. Non-stoichiometry arises due to the instability of nickel in the oxidation state Ni^{+3} at high temperature. Oxygen is detached (burned out) from nickel oxyhydroxide to form nickel oxyhydroxide with a mixed oxidation state [25]. The reduced form of nickel Ni^{2+} occupies lithium positions in the cathode material due to the similarity in ionic radii sizes [26].

Increasing the ratio of alkali metal cations to transition metals during synthesis leads to an increase in lithium content in the sample, likely due to shifting the equilibrium toward the formation of the final product with higher content of lithium ions in the structure of lithium nickelate. Increasing the content of lithium cations during the production of the target product during heat treatment helps stabilize the state of Ni^{3+} ions, preventing the "burning out" of oxygen from nickel oxyhydroxide and, as a result, the reduction of Ni^{3+} cations to Ni^{2+} , whose cations can occupy vacant positions instead of Li^+ ions. Thus, at a metal ratio of $2.5 : 1$, a sample with the composition $\text{Li}_{0.35}\text{Ni}_{1.65}\text{O}_2$ is formed, at a ratio of $5 : 1$ – $\text{Li}_{0.64}\text{Ni}_{1.36}\text{O}_2$, and the composition $\text{Li}_{0.98}\text{Ni}_{1.02}\text{O}_2$ is formed at a $\text{Li} : \text{Ni}$ ratio of 10 (Fig. 1a–1d, Table 1). It

has been experimentally shown that increasing the ratio of metal cations to 10 during the synthesis of target products contributes to the formation of a sample with almost stoichiometric composition.

To determine the influence of the time factor of heat treatment on the composition of synthesized compounds, the obtained collective precipitates were calcined at 700°C with a ratio of $\text{Li}^+ : \text{Ni}^{2+}$ equal to 10 (optimal ratio at which compounds close to stoichiometry are formed), for different periods of time. For convenience of research, a 15-minute step of thermal treatment of the collective precipitate was chosen. From Fig. 1g-1k and Table 1, it follows that during thermal treatment for 15 minutes, a sample with composition $\text{Li}_{0.524}\text{Ni}_{1.476}\text{O}_2$ is formed. Increasing the holding time under the same conditions promotes an increase in the content of lithium cations in the target product. With 30-minute heat treatment of the collective precipitate, a sample of composition $\text{Li}_{0.79}\text{Ni}_{1.21}\text{O}_2$ is formed, with 45-minute treatment - a compound of composition $\text{Li}_{0.92}\text{Ni}_{1.08}\text{O}_2$ is formed, and with one-hour heat treatment - a phase $\text{Li}_{0.98}\text{Ni}_{1.02}\text{O}_2$, in which the deviation from the stoichiometric composition is about 2% _{mol}. Apparently, the limiting factor in the formation of lithium nickelate with a short holding time is the slow diffusion of lithium in the formed melt (melting point of lithium hydroxide is 462°C [27]). Increasing the time of the second stage of synthesis (solid-phase completion) promotes greater and more complete interaction of lithium with nickel, in the case of holding for 1 hour.

It has been established that increasing the time of heat treatment in the second stage of synthesis of lithium nickelates to 1 hour promotes an increase in the content of Li^+ cations in the target product and ensures the formation of a product close to stoichiometry. Further increase in the temperature holding time will contribute to the intensification of the agglomeration process (enlargement) of product particles and decrease its specific surface area.

To establish the influence of the temperature factor on the composition of the target products obtained after evaporation of the suspension, the collective precipitates were calcined at different temperatures for one hour. As can be seen from Fig. 1d, 1h, 1i, 1j and Table 1, at 500°C and a 10-fold excess of lithium relative to nickel, a sample with the composition $\text{Li}_{0.55}\text{Ni}_{1.45}\text{O}_2$ is formed. With an increase in the process temperature, the content of lithium cations in the compounds increases, which is confirmed by the results of X-ray phase and chemical analysis methods. Thus, at a processing temperature of 550°C, lithium nickelate with the composition $\text{Li}_{0.68}\text{Ni}_{1.32}\text{O}_2$ is formed, at 600°C – $\text{Li}_{0.75}\text{Ni}_{1.25}\text{O}_2$, and at 700°C – $\text{Li}_{0.98}\text{Ni}_{1.02}\text{O}_2$, which is close to stoichiometry. The increase in the content of lithium cations in the target product with an increase in temperature from 500 to 700°C is apparently associated with an increase in the diffusion activity of lithium in the formed melt due to a probable decrease in its viscosity. Thus, it has been established that increasing the processing temperature to 700°C in the second stage of synthesis contributes to an increase in the content of lithium cations in the sample composition. A further increase in temperature will lead to the enlargement of product particles [28]. It has been experimentally established that with this approach to obtaining lithium nickelates close to stoichiometric composition, the main factors affecting the stability of Ni^{3+} cations at high temperatures are the molar ratio of lithium hydroxide and nickel, synthesis time, and processing temperature.

Fourier transform infrared spectra (FTIR) can be used to determine the crystal structure and molecular composition of stoichiometric or near-stoichiometric nanosized lithium nickelate samples [29]. Figure 2 shows the results of IR spectra analysis for a $\text{Li}_{0.98}\text{Ni}_{1.02}\text{O}_2$ sample, which has a composition close to stoichiometric. It can be seen that strong absorption peaks appear in the range of 500-1630 cm^{-1} . The absorption peaks at 505.4, 861.1, 1439.9, and 1503.5 cm^{-1} are typical for lithium nickelate with stoichiometric composition (LiNiO_2), which is consistent with the

data in [32], where it is stated that these absorption peaks can be used to identify stoichiometric lithium nickelate. The lithium nickelate crystal is a complex oxide compound in which a layer of Li ions is located between layers of Ni and O. The absorption peak at 505.4 cm^{-1} corresponds to the symmetric stretching and compression vibration peak of M-O-M (M = Li, Ni) [30, 31]. The peaks at 1439.9 and 1503.5 cm^{-1} are related to the bond energies of Ni-O and Ni=O, respectively. Their proximity is explained by the homogenization of valence electrons. The absorption bands observed in the range of $3400\text{--}3850 \text{ cm}^{-1}$ belong to the OH groups of water molecules [32].

Based on experimentally obtained data on the influence of synthesis conditions (ratio of Li^+ and Ni^{2+} , time and temperature factors) on the composition of materials based on lithium nickelate, a basic technological scheme has been created for obtaining these compounds close to the stoichiometric composition (Fig. 3), which is based on the operations indicated at the beginning of the section, as well as operations for processing washing solutions to obtain components for use in the synthesis of target products. For this purpose, it is proposed to carry out the following sequential operations. After washing the target product from the salts of the mother electrolyte and its separation by filtration from the collective solution (mixed solution of Li_2CO_3 and NaCl), it is necessary to introduce a solution of highly soluble sodium chloride into the latter for salting out the substantially less soluble lithium carbonate and separating the latter from the solution by filtration. The sodium chloride solution, after concentration adjustment, can be used again for salting out lithium carbonate.

It is proposed to dissolve the solid product Li_2CO_3 in a solution of hydrochloric acid to obtain a lithium chloride solution, which is then sent to electrodialysis to produce solutions of hydrochloric acid and lithium hydroxide. The HCl solution can

be reused for dissolving Li_2CO_3 , and the LiOH solution is directed to the head of the process.

The proposed closed technological scheme, namely the communication system of equipment, must be hermetically sealed in terms of leaks/and leakages of technological solutions, some of which are aggressive environments. Nickel cations precipitate from the initial solutions as completely as possible; after washing from the mother electrolyte, the solution may contain nickel cations only in trace amounts, close to the maximum permissible concentration values.

The uniqueness of the proposed developed basic technological scheme for the synthesis of cathode materials based on lithium nickelate close to the stoichiometric composition lies in the processing of the resulting technological solutions to obtain reagent solutions used in the same technology.

The carbon dioxide formed during the dissolution of lithium carbonate in hydrochloric acid at one of the stages of the basic technological scheme can be captured on filters. It can also be neutralized with water to form carbonic acid, which can subsequently be used in other technological processes, or react with calcium oxide to form calcium carbonate, which can also find application in various technological processes, etc.

Thus, the experimentally found conditions (time, temperature) allow obtaining cathode materials based on lithium nickelate, close to the stoichiometric composition of high frequency. The products obtained by this technology meet the requirements imposed on them. In addition, the reuse of reagents, reducing the technogenic load on the environment makes the proposed technology more preferable from the point of view of environmental safety. The proposed approach to synthesis, in contrast to existing solid-phase approaches, significantly reduces the energy costs for the production of target products and, as a consequence, the technogenic load on the environment.

In order to establish patterns of influence of composition (different content of lithium cations in $\text{Li}_{1-x}\text{Ni}_{1+x}\text{O}_2$) and synthesis conditions on the properties of synthesized lithium nickelates, two samples $\text{Li}_{0.79}\text{Ni}_{1.21}\text{O}_2$ and $\text{Li}_{0.98}\text{Ni}_{1.02}\text{O}_2$ were selected for the study. The choice of these samples is due to the fact that they can be used as cathode material in a lithium-ion battery, with one compound being close to stoichiometric composition by its composition, and the other compound having a relatively high lithium content with minimal synthesis time.

The structural characteristics of the phases were refined using the Whole Powder Pattern Fitting (WPPF) method of X-ray diffraction patterns. The criteria for R -factor were the values of profile R -factors R_p and R_{wp} , calculated using standard formulas. Table 2 presents the results of X-ray structural analysis of $\text{Li}_{0.98}\text{Ni}_{1.02}\text{O}_2$ and $\text{Li}_{0.79}\text{Ni}_{1.21}\text{O}_2$ samples. The WPPF refinement showed that the structure of the samples corresponds to a rhombohedral phase with SPGR $R\bar{3}m$ (166) symmetry.

The morphology of the synthesized samples was studied using SEM microscopy (Fig. 4). The obtained images were analyzed using ScanMaster software, which allows determining the granulometric composition. As can be seen from the analysis results (histogram inserts in Fig. 4), the particle size of the synthesized compounds $\text{Li}_{0.79}\text{Ni}_{1.21}\text{O}_2$ and $\text{Li}_{0.98}\text{Ni}_{1.02}\text{O}_2$ is non-uniform, but particles of predominantly one size (Table 2) prevail for each composition. The morphology of the particles is different. It can be assumed that the predominance of one particle size and well-developed specific surface area may have a positive effect on the electrochemical properties of cathode materials based on lithium nickelates for lithium-ion batteries.

Table 3 presents the values of the specific surface area for the indicated sample compositions, determined by the BET method from nitrogen sorption/desorption isotherms using a TriStar II 3020 electronic specific surface area analyzer. Thermal treatment of $\text{Li}_{0.98}\text{Ni}_{1.02}\text{O}_2$ at 700°C for 1 hour ensures the formation of nanosized

compounds with a developed specific surface area. Meanwhile, the 30-minute exposure of $\text{Li}_{0.79}\text{Ni}_{1.21}\text{O}_2$ did not allow the formation of smaller nanosized particles (Table 3, Fig. 4). Thus, the specific surface area of the $\text{Li}_{0.79}\text{Ni}_{1.21}\text{O}_2$ compound is smaller than that of $\text{Li}_{0.98}\text{Ni}_{1.02}\text{O}_2$.

The sample with increased lithium content has a more developed surface and smaller particle size compared to the sample containing a smaller amount of Li^+ cations (Table 3, Fig. 4).

Fig. 5 and 6 show impedance hodographs for $\text{Li}_{0.79}\text{Ni}_{1.21}\text{O}_2$ and $\text{Li}_{0.98}\text{Ni}_{1.02}\text{O}_2$ respectively. It can be seen that the complex $Z''Z'$ diagrams of impedance are qualitatively similar. They reveal a high-frequency Debye-type relaxation process in the form of a semicircle arc and a low-frequency process in the form of an inclined line.

In the high-frequency region of the spectrum, the impedance hodographs have the form of a distorted semicircle with a center located below the abscissa axis (Fig. 5, 6), which is due to a parallel RC connection. The distorted semicircle can be modeled by various equivalent circuits [33-35]. We chose the circuit shown in Fig. 7, as it most accurately reflects the physical nature of the processes and satisfactorily models the experimental hodographs. This equivalent circuit was used to describe the impedance spectrum of the lithium electrode in studies [36, 37]. The choice of a circuit with Warburg impedance is justified for the spectra under consideration, since the initial part of the high-frequency region is linear in a small interval, which is characteristic of diffusion processes. The low-frequency region of the impedance hodograph spectrum, in the form of an inclined line, is modeled by a constant phase element (CPE) and is associated with the formation of a double electric layer at the sample-electrode interface.

We believe that the high-frequency arc reflects processes occurring in the bulk of the studied samples, while the low-frequency arc is associated with processes in

the near-electrode region. Additionally, from Fig. 5, 6 it can be seen that the semicircles do not start from zero, which indicates the presence of frequency-independent conductivity (probably provided by free electrons). The resistance R_s (Fig. 7) is responsible for modeling this conductivity.

The parameters of the impedance diagram processing results, using the EIS Spectrum Analyser software, are shown in Fig. 5, 6 (as lines) and in Table 4. It can be seen that the calculated curves correlate well with the experimental data.

When comparing the values given in Table 4, it is evident that the intrinsic specific ionic conductivity σ_{ct} of $\text{Li}_{0.98}\text{Ni}_{1.02}\text{O}_2$ (700°C, 60 min) is 2.5 times higher compared to $\text{Li}_{0.79}\text{Ni}_{1.21}\text{O}_2$ (700°C, 45 min). This is likely due to the greater number of charge carriers ($\text{Li}_{0.98}$ vs $\text{Li}_{0.79}$) (consistent with work [38]) and more developed specific surface area. It can be assumed with a high degree of probability that samples synthesized at lower temperatures and containing fewer lithium cations as charge carriers will have worse electrochemical characteristics compared to samples that are close to stoichiometric composition.

Further research necessary for optimizing the synthesis of LiNiO_2 and improving its properties will be related to studying the main parameters for evaluating stability (degradation) and durability of LiNiO_2 under real battery operating conditions, which include recharging cycles in discharge-charge mode at various current strengths, which will determine the service life (stability and durability) of these electrode materials.

CONCLUSION

For the first time, a new method for producing lithium nickelate cathode materials has been proposed, the peculiarity of which lies in using two technological approaches: sol-gel and solid-phase synthesis. The developed technological scheme

allows for avoiding the use of expensive precursors and employs less energy-intensive synthesis conditions. Thanks to this approach, it was possible to obtain nanosized powders of $\text{Li}_{0.98}\text{Ni}_{1.02}\text{O}_2$, close to stoichiometric composition.

The influence of the ratio of lithium and nickel cations during synthesis on the composition of the final product has been established. At a ratio of $\text{Li}^+ : \text{Ni}^{2+}$ less than 10:1, a lithium-depleted phase is formed. Increasing the ratio of alkali cations to transition metal promotes an increase in lithium content in the sample as a result of shifting the equilibrium towards the formation of the final product.

The influence of thermal treatment time on the composition of lithium nickelate is shown. It is established that the optimal synthesis time is 1 hour, as shorter thermal treatment time leads to the formation of a final product depleted in Li^+ cation content. Further increase in temperature holding time promotes intensification of particle agglomeration process and reduces the specific surface area of the final product particles.

The influence of the temperature factor of the second synthesis stage on the composition of target products is determined. Despite a 10-fold excess of lithium relative to nickel, at temperatures below 700°C, a composition depleted in Li^+ cation content is formed. Thus, 700°C is the optimal synthesis temperature, which ensures the formation of a product close to stoichiometry. Non-stoichiometry occurs due to the instability of nickel in the oxidation state Ni^{3+} at high temperature. It is established that thermal treatment at 700°C for 1 hour ensures the formation of nanosized compounds with a developed specific surface area, while reducing the holding time does not contribute to the formation of smaller nanosized particles.

The electrochemical properties of some compositions close to stoichiometric ones were studied by impedance spectroscopy. The electrochemical characteristics of cathode materials are determined. It was revealed that a sample with a composition close to stoichiometric (LiNiO_2) demonstrates greater intrinsic specific ionic

conductivity σ_{ct} . This is probably due to a larger number of charge carriers and a more developed specific surface area. The experimentally obtained electrochemical characteristics of this sample are comparable with the electrochemical properties of lithium nickelates of stoichiometric composition obtained by other methods.

In addition, when obtaining the final product, it is proposed to process and regenerate used solutions and salts in order to return them to certain stages of the technological scheme. Minimization of waste, reuse of reagents, reduction of technogenic load on the environment makes the proposed technology more preferable from an environmental point of view.

FUNDING

The synthesis of materials was carried out within the framework of the state assignment of Sakhalin State University No. FEFF-2024-0001. Electrochemical studies were performed within the framework of the state research assignment FMEZ 2022-0015.

CONFLICT OF INTEREST

The authors declare no conflict of interest

REFERENCES

1. *Collins D.H.* // J. Power Sources. 1994. V. 52. № 2. P. 313. [https://doi.org/10.1016/0378-7753\(94\)87026-8](https://doi.org/10.1016/0378-7753(94)87026-8)
2. *Ohzuku T. , Ueda A. , Nagayama M.* // J. Electrochem. Soc. 1993. V. 140. № 7. P. 1862. <https://doi.org/10.1149/1.2220730>
3. *Kalaiselvi N., Periasamy P., Thirunakaran R. et al.* // Ionics (Kiel) 2001. V. 7. № 4–6. P. 451. <https://doi.org/10.1007/BF02373583>

4. *Minakshi M., Sharma N., Ralph D. et al.* // *Electrochem. Solid-State Let.* 2011. V. 14. № 6. P. A86. <https://doi.org/10.1149/1.3561764>
5. *Divakaran A.M., Minakshi M., Bahri P.A. et al.* // *Progr. Solid State Chem.* 2021. V. 62. P. 100298. <https://doi.org/10.1016/j.progsolidstchem.2020.100298>
6. *Wang R.-C. , Lin Y.-C. , Wu S.-H.* // *Hydrometallurgy.* 2009. V. 99. № 3–4. P. 194. <https://doi.org/10.1016/j.hydromet.2009.08.005>
7. *Monajjemi M., Mollaamin F., Thu P.T. et al.* // *Russ. J. Electrochem.* 2020. V. 56. № 8. P. 669. <https://doi.org/10.1134/S1023193520030076>
8. *Sivajee Ganesh K., Purusottam Reddy B., Jeevan Kumar P. et al.* // *J. Electroanalyst. Chem.* 2018. V. 828. P. 71. <https://doi.org/10.1016/j.jelechem.2018.09.032>
9. *Kalyani P.* // *J. Power Sources.* 2002. V. 111. № 2. P. 232. [https://doi.org/10.1016/S0378-7753\(02\)00307-5](https://doi.org/10.1016/S0378-7753(02)00307-5)
10. *Ramesh Babu B., Periasamy P., Thirunakaran R. et al.* // *Int. J. Inorg. Mater.* 2001. V. 3. № 4–5. P. 401. [https://doi.org/10.1016/S1466-6049\(01\)00023-X](https://doi.org/10.1016/S1466-6049(01)00023-X)
11. *Thirunakaran R., Kalaiselvi N., Periasamy P. et al.* // *Ionics (Kiel).* 2001. V. 7. № 3. P. 187. <https://doi.org/10.1007/BF02419227>
12. *Bianchini M., Roca-Ayats M., Hartmann P. et al.* // *Angewandte Chem. Int. Edit.* 2019. V. 58. № 31. P. 10434. <https://doi.org/10.1002/anie.201812472>
13. *Hata M., Tanaka T., Kato D. et al.* // *Electrochem.* 2021. V. 89. № 3. P. 223. <https://doi.org/10.5796/electrochemistry.20-65151>
14. *Tolganbek N., Yerkinbekova Y., Kalybekkyzy S. et al.* // *J. Alloys Compd.* 2021. V. 882. P. 160774. <https://doi.org/10.1016/j.jallcom.2021.160774>
15. *Shembel' E.M., Apostolova R.D., Aurbach D. et al.* // *Russ. J. App. Chem.* 2014. V. 87. № 9. P. 1260. <https://doi.org/10.1134/S1070427214090122>
16. *Wang L., Chen B., Ma J. et al.* // *Chem. Soc. Rev.* 2018. V. 47. № 17. P. 6505. <https://doi.org/10.1039/C8CS00322J>
17. *Divakaran A.M., Minakshi M., Bahri P.A. et al.* // *Progress Solid State Chem.* 2021. V. 62. P. 100298. <https://doi.org/10.1016/j.progsolidstchem.2020.100298>
18. *Kalyani P. , Kalaiselvi N.* // *Sci. Technol. Adv. Mater.* 2005. V. 6. № 6. P. 689. <https://doi.org/10.1016/j.stam.2005.06.001>

19. *Kalyani P. , Kalaiselvi N. , Renganathan N.G.* // J. Power Sources. 2003. V. 123. № 1. P. 53. [https://doi.org/10.1016/S0378-7753\(03\)00458-0](https://doi.org/10.1016/S0378-7753(03)00458-0)
20. *Kalyani P., Kalaiselvi N., Renganathan N.G. et al.* // Mater. Res. Bull. 2004. V. 39. № 1. P. 41. <https://doi.org/10.1016/j.materresbull.2003.09.021>
21. *Mesnier A. , Manthiram A.* // ACS Appl. Mater. Interfaces. 2020. V. 12. № 47. P. 52826. <https://doi.org/10.1021/acsami.0c16648>
22. *Välikangas J., Laine P., Hietaniemi M. et al.* // Appl. Sci. 2020. V. 10. № 24. P. 8988. <https://doi.org/10.3390/app10248988>
23. *Bianchini M., Fauth F., Hartmann P. et al.* // J. Mater. Chem. A. Mater. 2020. V. 8. № 4. P. 1808. <https://doi.org/10.1039/C9TA12073D>
24. *Pesterfield L.* // J. Chem. Educ. 2009. V. 86. № 10. P. 1182. <https://doi.org/10.1021/ed086p1182>
25. *Tretyakov Yu.D., Martynenko L.I., Grigoriev A.N., Tsivadze A.Yu.* // Inorg. Chem. 2001. V. 1. P. 378.
26. *Makhonina E.V. , Pervov V.S. , Dubasova V.S.* // Russ. Chem. Rev. 2004. V. 73. № 10. P. 991. <https://doi.org/10.1070/RC2004v073n10ABEH000896>
27. *Rabinovich V.A., Khavik E.Ya.* Brief Chemical Handbook. L.: Chemistry, 1978. 334 p.
28. *Riewald F., Kurzhals P., Bianchini M. et al.* // J. Electrochem. Soc. 2022. V. 169. № 2. P. 020529. <https://doi.org/10.1149/1945-7111/ac4bf3>
29. *Taha T.A. , El-Molla M.M.* // J. Mater. Res. Technol. 2020. V. 9. № 4. P. 7955. <https://doi.org/10.1016/j.jmrt.2020.04.098>
30. *Yan F.Y. , Zhang H. , Lai Q.* // J. Sichuan University. 2002. V. 39. P. 918.
31. *Ohzuku T., Ueda A., Nagayama M. et al.* // Electrochim. Acta. 1993. V. 38. № 9. P. 1159. [https://doi.org/10.1016/0013-4686\(93\)80046-3](https://doi.org/10.1016/0013-4686(93)80046-3)
32. *Taha T.A. , Elrabaie S. , Attia M.T.* // J. Mater. Sci.: Mater. Electronics. 2018. V. 29. № 21. P. 18493. <https://doi.org/10.1007/s10854-018-9965-4>
33. *Levi M.D. , Aurbach D.* // J. Phys. Chem. B. 2004. V. 108. № 31. P. 11693. <https://doi.org/10.1021/jp0486402>
34. *Umeda M., Dokko K., Fujita Y. et al.* // Electrochim. Acta. 2001. V. 47. № 6. P. 885. [https://doi.org/10.1016/S0013-4686\(01\)00799-X](https://doi.org/10.1016/S0013-4686(01)00799-X)

35. *Wang C. , Appleby A.J. , Little F.E. // Electrochim. Acta. 2001. V. 46. № 12. P. 1793. [https://doi.org/10.1016/S0013-4686\(00\)00782-9](https://doi.org/10.1016/S0013-4686(00)00782-9)*
36. *Ivanishchev A.V., Gridina N.A., Rybakov K.S. et al. // J. Electroanalytical Chem. 2020. V. 860. P. 113894. <https://doi.org/10.1016/j.jelechem.2020.113894>*
37. *Churikov A.V., Ivanishchev A.V., Zapsis K.V. et al. // Electrochemical Energetics. 2007. V. 7. № 4. P. 169.*
38. *Amin R. , Ravnsbæk D.B. , Chiang Y.-M. // J. Electrochem. Soc. 2015. V. 162. № 7. P. A1163. <https://doi.org/10.1149/2.0171507jes>*

Table 1. Chemical and phase composition of lithium nickelate-based compounds depending on synthesis conditions

Sample No.	Li : Ni ratio, mol.	Heat treatment conditions		Composition, wt. %		XRD Phase	Database card No.
		τ , min	T, °C	Li	Ni		
1	1.5 : 1	60	700	1.26	75.28	$\text{Li}_{0.25}\text{Ni}_{1.75}\text{O}_2$	04-012-0769
2	2.5 : 1	60	700	1.84	73.78	$\text{Li}_{0.35}\text{Ni}_{1.65}\text{O}_2$	04-021-2225
3	5 : 1	60	700	3.80	68.67	$\text{Li}_{0.64}\text{Ni}_{1.36}\text{O}_2$	04-007-6320
4	10 : 1	60	700	6.86	60.70	$\text{Li}_{0.98}\text{Ni}_{1.02}\text{O}_2$	04-012-6498
5	10 : 1	15	700	2.96	70.87	$\text{Li}_{0.524}\text{Ni}_{1.476}\text{O}_2$	01-089-3603
6	10 : 1	30	700	5.05	65.45	$\text{Li}_{0.79}\text{Ni}_{1.21}\text{O}_2$	01-089-3602
7	10 : 1	45	700	6.24	62.31	$\text{Li}_{0.92}\text{Ni}_{1.08}\text{O}_2$	04-007-6736
8	10 : 1	60	500	3.15	85.10	$\text{Li}_{0.55}\text{Ni}_{1.45}\text{O}_2$	04-021-2223
9	10 : 1	60	550	4.13	67.84	$\text{Li}_{0.68}\text{Ni}_{1.32}\text{O}_2$	01-088-1605
10	10 : 1	60	600	4.68	66.37	$\text{Li}_{0.75}\text{Ni}_{1.25}\text{O}_2$	04-006-8817

Table 2 . Refined unit cell parameters of $\text{Li}_{0.98}\text{Ni}_{1.02}\text{O}_2$ and $\text{Li}_{0.79}\text{Ni}_{1.21}\text{O}_2$

Parameter	$\text{Li}_{0.98}\text{Ni}_{1.02}\text{O}_2$	$\text{Li}_{0.79}\text{Ni}_{1.21}\text{O}_2$
a , b , Å	2.88868(8)	2.90003(8)
c , Å	14.2167(6)	14.2590(7)
α, β , deg	90.000	90.000
γ , deg	120.000	120.000
V , Å ³	102.737	103.854
R_{wp} , %	12.57	12.66
R_p , %	9.34	9.44
Sp. gr.	$\text{R } \bar{3} \text{ m}$	$\text{R } \bar{3} \text{ m}$

Table 3. Physical parameters of synthesized compounds based on lithium nickelates

Sample composition	Heat treatment, °C	Physical parameters	
		S_{sp} , m ² /g	D , nm
$\text{Li}_{0.79}\text{Ni}_{1.21}\text{O}_2$	700	17.44	420
$\text{Li}_{0.98}\text{Ni}_{1.02}\text{O}_2$	700	22.85	190

Table 4. Parameters of the equivalent circuit obtained by modeling impedance spectra of $\text{Li}_{1+x}\text{Ni}_{1+x}\text{O}_2$

Composition	R_s , Ohm	R_{ct} , Ohm	C_{ct} , F	W_{ct} , Ohm/s _{1/2}	C_{dl} , F	n_{dl}	σ_s , S/m	σ_{ct} , S/m
$\text{Li}_{0.98}\text{Ni}_{1.02}\text{O}_2$	31.02	257.43	4.617×10^{-10}	0.995×10^{-6}	3.429×10^{-6}	0.6908	0.406	0.049
$\text{Li}_{0.79}\text{Ni}_{1.21}\text{O}_2$	22.896	644.8	5.032×10^{-10}	1.355×10^{-6}	2.513×10^{-6}	0.7339	0.55	0.0197

Fig. 1. X-ray diffraction patterns of samples: a – $\text{Li}_{0.25}\text{Ni}_{1.75}\text{O}_2$, b – $\text{Li}_{0.35}\text{Ni}_{1.65}\text{O}_2$, c – $\text{Li}_{0.64}\text{Ni}_{1.36}\text{O}_2$, d – $\text{Li}_{0.98}\text{Ni}_{1.02}\text{O}_2$, e – $\text{Li}_{0.524}\text{Ni}_{1.476}\text{O}_2$, f – $\text{Li}_{0.79}\text{Ni}_{1.21}\text{O}_2$, g – $\text{Li}_{0.92}\text{Ni}_{1.08}\text{O}_2$, h – $\text{Li}_{0.55}\text{Ni}_{1.45}\text{O}_2$, i – $\text{Li}_{0.68}\text{Ni}_{1.32}\text{O}_2$, j – $\text{Li}_{0.75}\text{Ni}_{1.25}\text{O}_2$.

Fig. 2. IR spectra of the sample with composition $\text{Li}_{0.98}\text{Ni}_{1.02}\text{O}_2$.

Fig. 3. Principal technological scheme for obtaining lithium nickelate.

Fig. 4. SEM images of samples: $\text{Li}_{0.79}\text{Ni}_{1.21}\text{O}_2$ (a); $\text{Li}_{0.98}\text{Ni}_{1.02}\text{O}_2$ (b).

Fig. 5. Complex impedance diagram of $\text{Li}_{0.79}\text{Ni}_{1.21}\text{O}_2$.

Fig. 6. Complex impedance diagram of $\text{Li}_{0.98}\text{Ni}_{1.02}\text{O}_2$.

Fig. 7. Equivalent circuit diagram.

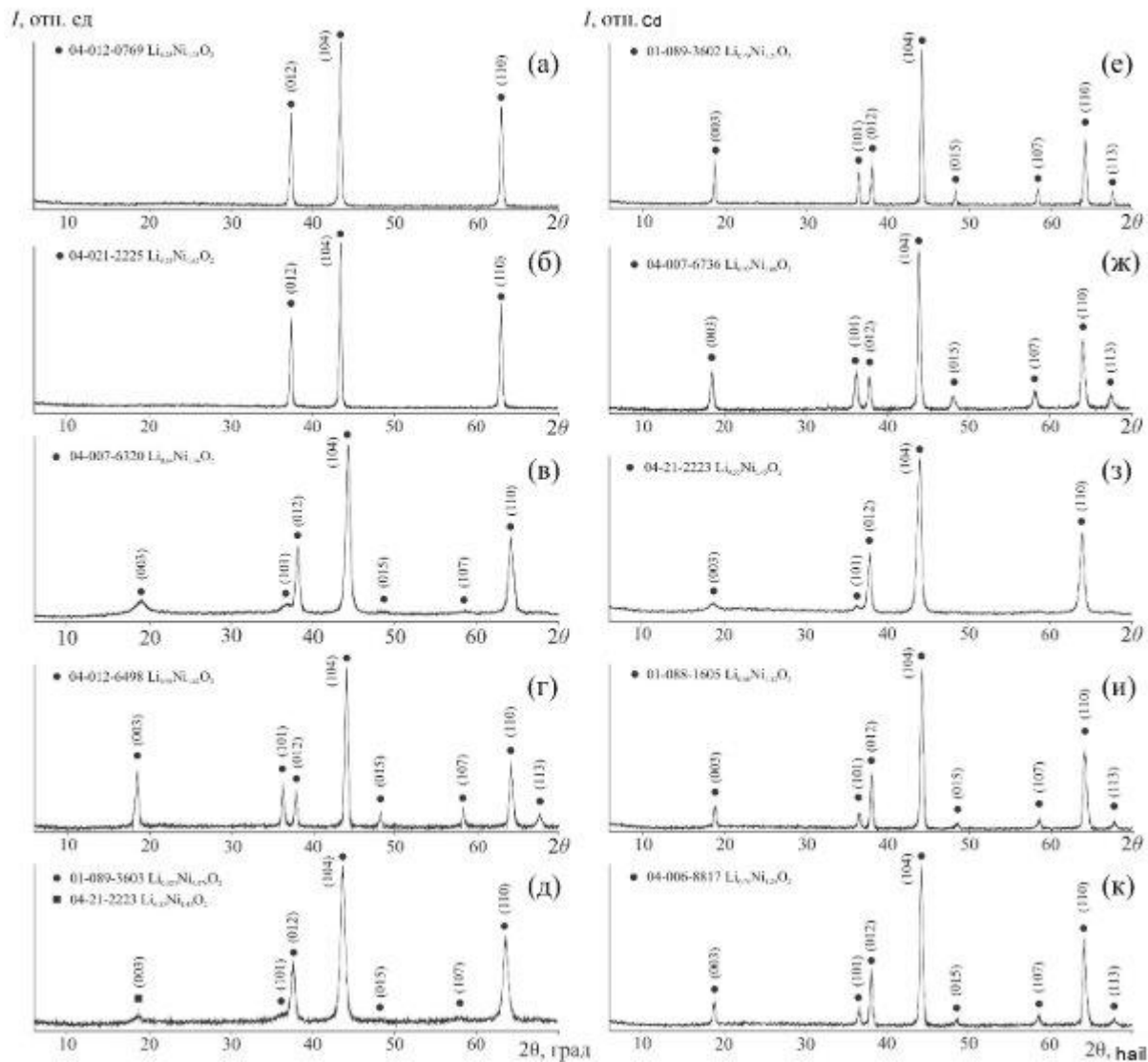


Fig. 1. Korneykov et al.

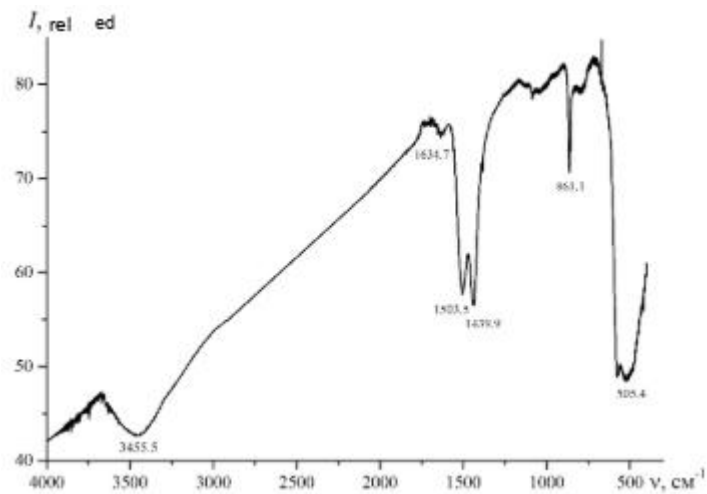


Fig. 2. Korneykov et al.

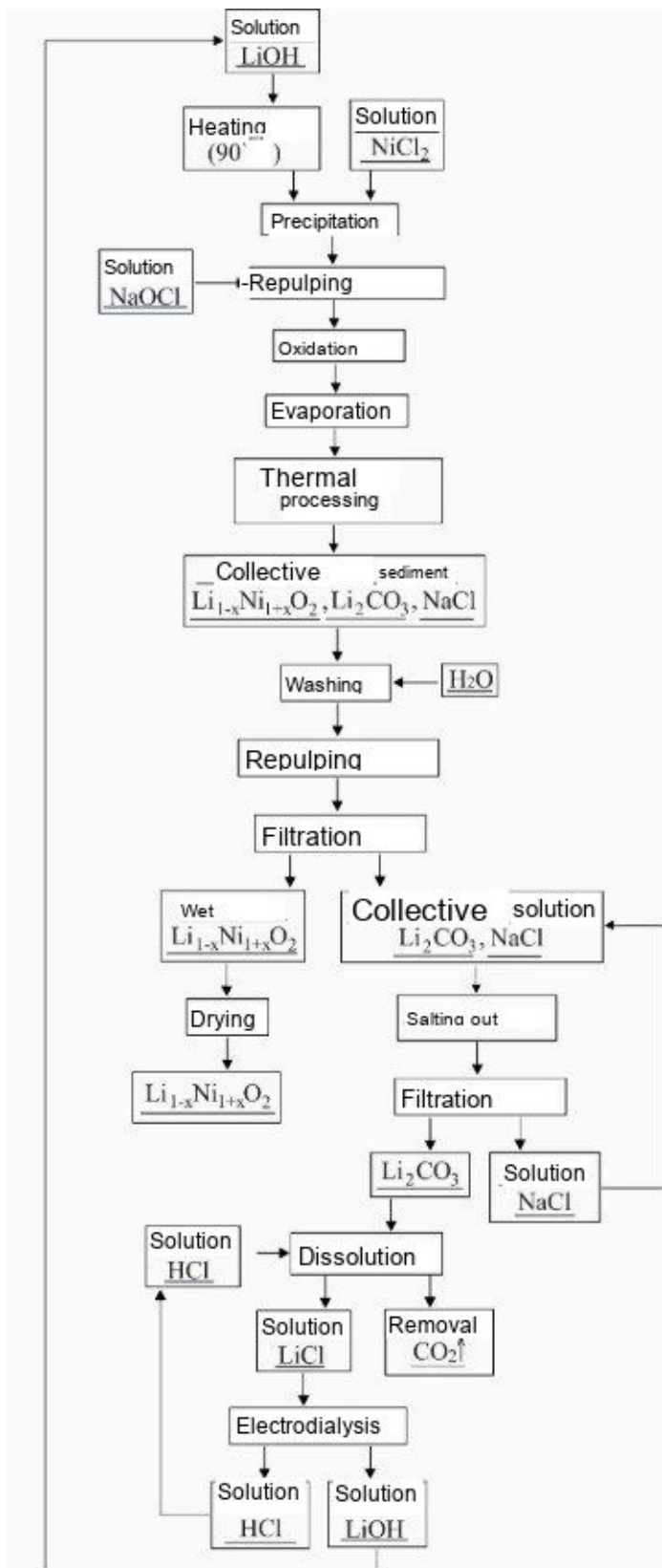


Fig. 3. Korneykov et al.

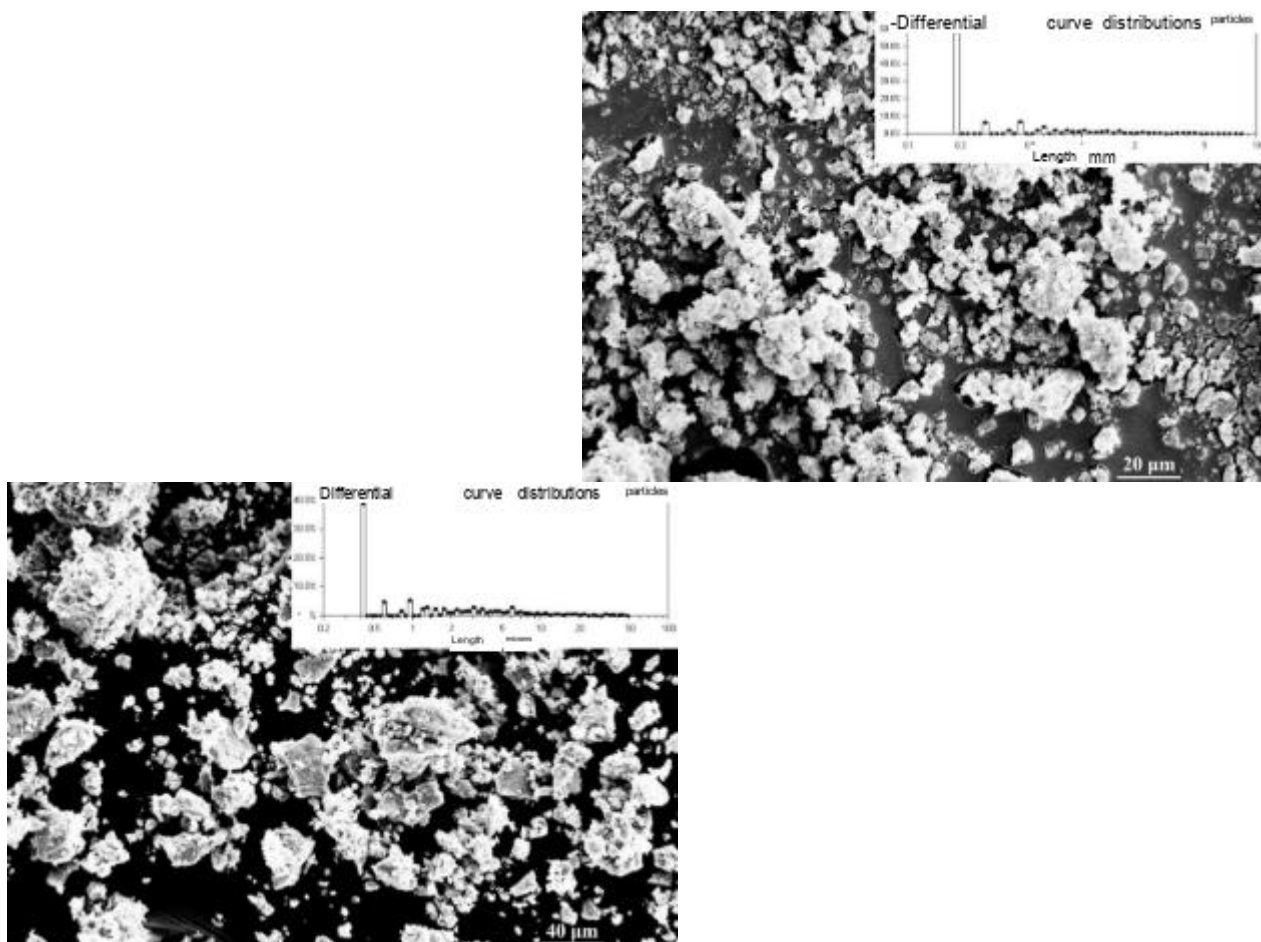


Fig. 4. Korneykov et al.

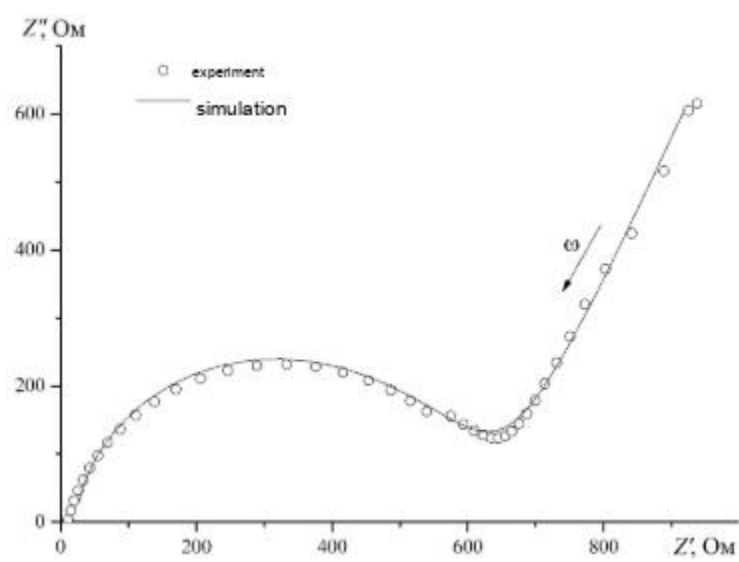


Fig. 5. Korneykov et al.

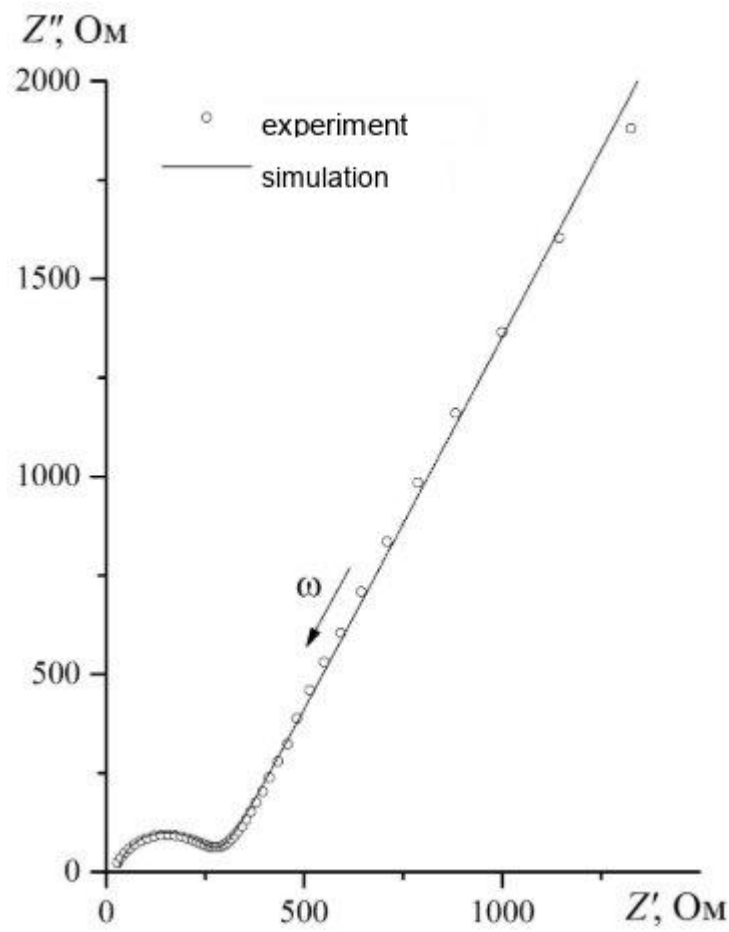


Fig. 6. Korneykov et al.

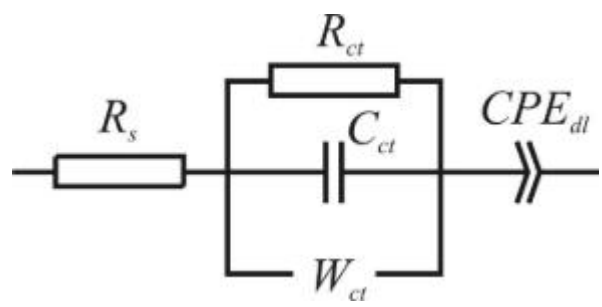


Fig. 7. Korneykov et al.